

See discussions, stats, and author profiles for this publication at: <https://www.researchgate.net/publication/263944664>

New Organic Dyes with a Phenanthrenequinone Derivative as the π -Conjugated Bridge for Dye-Sensitized Solar Cells

ARTICLE in THE JOURNAL OF PHYSICAL CHEMISTRY C · JUNE 2013

Impact Factor: 4.77 · DOI: 10.1021/jp400011w

CITATIONS

12

READS

10

5 AUTHORS, INCLUDING:



Xichuan Yang

Dalian University of Technology

73 PUBLICATIONS 2,577 CITATIONS

SEE PROFILE



Ming Cheng

KTH Royal Institute of Technology

32 PUBLICATIONS 484 CITATIONS

SEE PROFILE

New Organic Dyes with a Phenanthrenequinone Derivative as the π -Conjugated Bridge for Dye-Sensitized Solar Cells

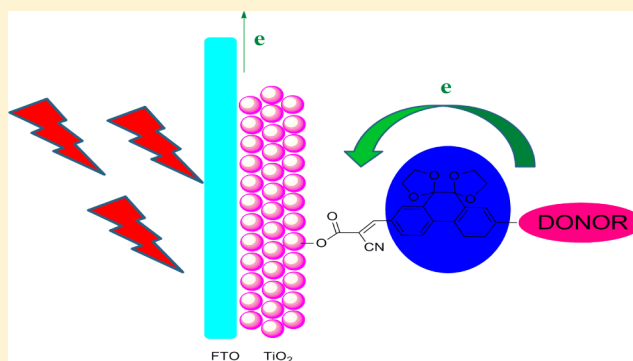
Jianghua Zhao,[†] Xichuan Yang,^{*,†} Ming Cheng,[†] Shifeng Li,[†] and Licheng Sun^{*,†,‡}

[†]State Key Laboratory of Fine Chemicals, DUT–KTH Joint Education and Research Centre on Molecular Devices, Dalian University of Technology (DUT), 2 Linggong Road, 116024 Dalian, China

[‡]School of Chemical Science and Engineering, Centre of Molecular Devices, Department of Chemistry, KTH Royal Institute of Technology, Teknikringen 30, 10044 Stockholm, Sweden

S Supporting Information

ABSTRACT: A series of organic dyes based on a phenanthrenequinone derivative have been employed for the first time as a π -conjugated bridge in the molecular design of D- π -A structured organic dyes. Photophysical and electrochemical properties of dyes JH201–JH203 have been systematically investigated. The result shows that dye JH202 exhibits a higher molar extinction coefficient and widened absorption spectrum than dye JH201. Upon replacing the butoxytriphenylamine electron donor with phenothiazine, a bathochromic shift absorption spectrum for dye JH203 was observed. When applied in dye-sensitized solar cells (DSSCs), the device sensitized by JH203 yields the best photo-to-current conversion efficiency of 6.0% under standard AM 1.5G illumination (100 mW/cm²) with a short-circuit photocurrent density (J_{sc}) of 11.1 mA/cm², an open-circuit photovoltage (V_{oc}) of 720 mV, and a fill factor (Φ) of 74.9%. The maximum incident photo-to-current conversion efficiency reaches 87% at 460 nm.



INTRODUCTION

Dye-sensitized solar cells (DSSCs) have attracted significant attention as a new-generation photovoltaic (PV) device since Grätzel and O'Regan reported them in 1991.¹ There are three main components in DSSCs: anode, photosensitizer, and counter electrode. The photosensitizer plays a crucial role in the working process of the DSSCs. It absorbs photons and injects electrons to the conduction band (E_{cb}) of TiO₂. Then the oxidized dyes are regenerated by the electrolyte. Metal complexes such as N719, FT89, and YD2-o-C8 have obtained extremely high photon-to-electron conversion efficiency of exceeding 10%.^{2–4} Although, compared to metal complexes, D- π -A structured metal-free organic dyes exhibit poorer photovoltaic performance, they have still been paid more attention for their unique advantages such as low cost, being environmentally friendly, a higher molar extinction coefficient, and an adjustable structure. To date, the efficiencies of this kind of organic dye have been improved in the range of 7–10%.^{5–7} For D- π -A structured organic dyes, triphenylamine,^{8–10} phenothiazine,¹¹ coumarin,^{12–14} and indoline^{15–17} have been successfully used as electron donors. Also, for all of these dyes, cyanoacrylic acid has served as an electron acceptor. A π -conjugated bridge is used as a linker to connect the electron donor and electron acceptor together. Phenyl, thiophene, and its derivatives^{18,19} are generally used as π -conjugated bridges in molecular design of D- π -A structured organic dyes.

The structure of the organic dyes shows a great impact on the performance of the DSSCs. To obtain a high efficiency, two main strategies can be employed in the design of the organic dyes:²⁰ (1) reducing the energy gap (ΔE_g) of the dye molecule to match the electronic absorption spectrum with the standard solar emission spectrum for a higher photocurrent; (2) changing the steric structure of the dye to modulate the recombination in the TiO₂/dye/electrolyte surface for a high open-circuit photovoltage. To narrow ΔE_g , one common tactic is employing a strong electron donor or strong electron acceptor. Another strategy is to diminish rotation of the molecule for enhancing the delocalization of π -electrons. To diminish the rotation of the molecule, it is a good choice to adopt a rigid π -conjugated bridge.

In this work, a phenanthrenequinone derivative with a rigid conjugated structure, which is beneficial to suppression of rotation in the dye molecule for better delocalization of π -electrons, has been employed as a π -conjugated bridge for the first time in a JH series of D- π -A organic dyes JH201, JH202, and JH203 (seen in Figure 1). For dye JH201, a butoxytriphenylamine unit serves as an electron donor, and a traditional cyanoacetic acid unit is used as an electron acceptor.

Received: January 1, 2013

Revised: April 22, 2013

Published: April 26, 2013

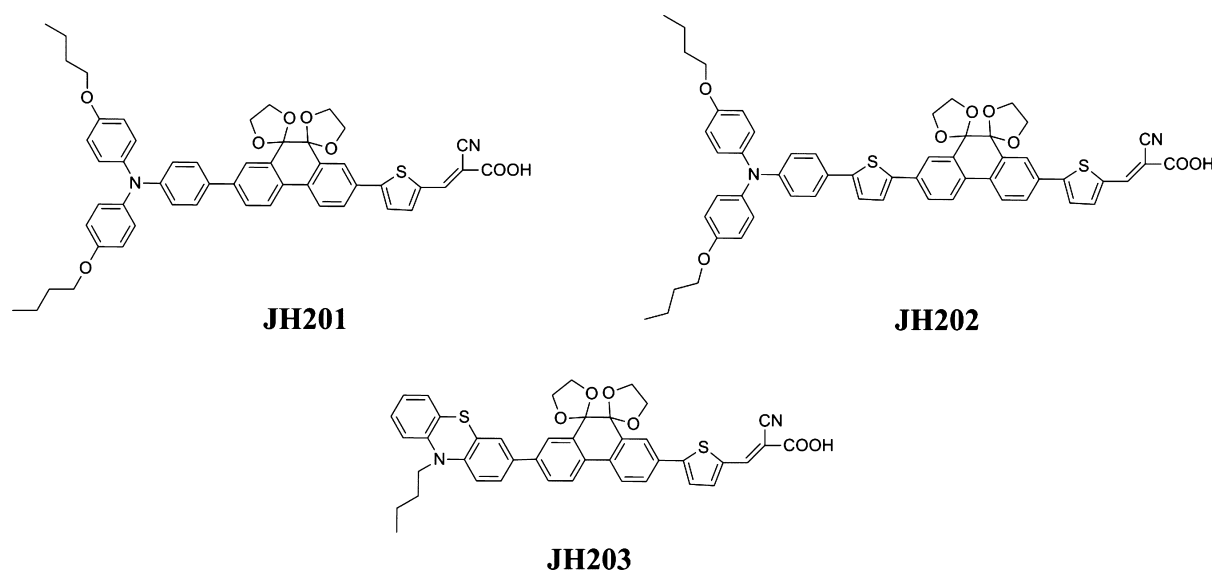


Figure 1. Structures of the sensitizers **JH201**–**JH203**.

Gaussian calculation studies have indicated that there is a large rotation between the butoxytriphenylamine rigid unit and the phenanthrenequinone derivative rigid unit, and the dye **JH202** has been designed to diminish this impact. To decrease the ΔE_g leading to a higher photocurrent and further understanding of the influence of different electron donors on the performance of the phenanthrenequinone derivative dyes, dye **JH203** with a phenothiazene moiety as the electron-donating group was synthesized for comparison. The specific synthetic routes are given in the Supporting Information. The performance of **JH** series of the dyes with different structures have been systematically investigated by photophysical, photovoltaic, and electrochemical methods.

EXPERIMENTAL SECTION

Analytical Measurements. The absorption spectra were recorded on HP8453 (USA). Electrochemical redox potentials were obtained by cyclic voltammetry (CV) on an electrochemistry workstation (BAS100B, USA). A traditional three-electrode system was used. The working electrode, auxiliary electrode, and reference electrode are a glassy carbon disk electrode, Pt wire, and Ag/Ag⁺ electrode, respectively. The photocurrent–voltage (*J*–*V*) properties were measured under AM 1.5G illumination (16S–002, Solar Light Co. Ltd., USA). The incident light intensity was 100 mW/cm² calibrated with a standard Si solar cell. The working areas of the cells were masked to 0.159 cm². The *J*–*V* data were collected by an electrochemical workstation (LK9805, Lanlike Co. Ltd., China). The measurement of the incident photo-to-current conversion efficiency (IPCE) was obtained by a Hypermono–light (SM–25, Jasco Co. Ltd., Japan).

Electrochemical impedance spectroscopy (EIS) was measured with an impedance/gain–phase analyzer (PARSTAT 2273, USA) under dark conditions, with a forward bias of –0.7 V. The alternating current (AC) amplitude was set at 10 mV.

Preparation of the DSSCs. The DSSCs sensitized by **JH201**–**JH203** were fabricated by modifying the previous report.²¹ A layer of 2 μm TiO₂ (13 nm paste, Heptachroma, China) was coated onto the F-doped tin oxide conducting glass (TEC15, 15 Ω/square, Pilkington, USA) by screen printing and then dried for 5 min at 120 °C. This procedure was repeated 5

times (10 μm), and a final coating of (4 μm) of TiO₂ paste (DHS–SLP1, Heptachroma, China) as the scattering layer was then applied. The double-layer TiO₂ electrodes (area: 6 × 6 mm) were sintered under an air flow at 500 °C for 60 min and then cooled to room temperature. The sintered film was further treated with 40 mM TiCl₄ aqueous solution at 70 °C for 30 min, then washed with water, and sintered at 500 °C for 60 min. After the film was cooled to room temperature, it was immersed into a 2 × 10^{–4} M dye bath for 12 h. The electrode was then rinsed with ethanol and dried. The hermetically sealed cells were fabricated by assembling the dye-loaded film as the working electrode and Pt-coated conducting glass as the counter electrode separated with a Surlyn 1702 film (60 μm, Dupont).

RESULTS AND DISCUSSION

Photophysical and Electrochemical Properties. The UV–visible absorption spectra of the **JH** series of the dyes in CH₂Cl₂ solution are shown in Figure 3(a), and the corresponding photophysical data are listed in Table 1. As is shown in Figure 3(a), dye **JH201** exhibits the absorption wavelength at 418 nm, which can be assigned to the S₀→S₁

Table 1. Absorption and Electrochemical Data of the **JH** Series of the Dyes

dye	absorption			oxidation potential		
	λ_{\max}^a (nm)	ϵ at λ_{\max}^a (M ^{–1} cm ^{–1})	λ_{\max}^b on TiO ₂ (nm)	E_{0-0}^c (V)	E_{ox}^d (V) (vs NHE)	E_{LUMO}^e (V) (vs NHE)
JH201	418	30155	398	2.51	0.71	–1.80
JH202	420	45105	400	2.41	0.67	–1.74
JH203	460	29085	431	2.33	0.77	–1.51

^aAbsorption spectra in solution were measured in CH₂Cl₂ solution (2 × 10^{–5} M). ^bAbsorption spectra on TiO₂ films were measured with dye-loaded TiO₂ films immersed in CH₂Cl₂ solution (2 × 10^{–5} M). ^c E_{0-0} was determined from intersection of the tangent of absorption on TiO₂ film and the *x*-axis by 1240/λ. ^dThe oxidation potentials of the dyes were measured in CH₂Cl₂ solutions with TBAPF₆ (0.1 M) as electrolyte and ferrocene/ferrocenium (F_c/F_c⁺) as an internal reference and converted to NHE by addition of 440 mV.

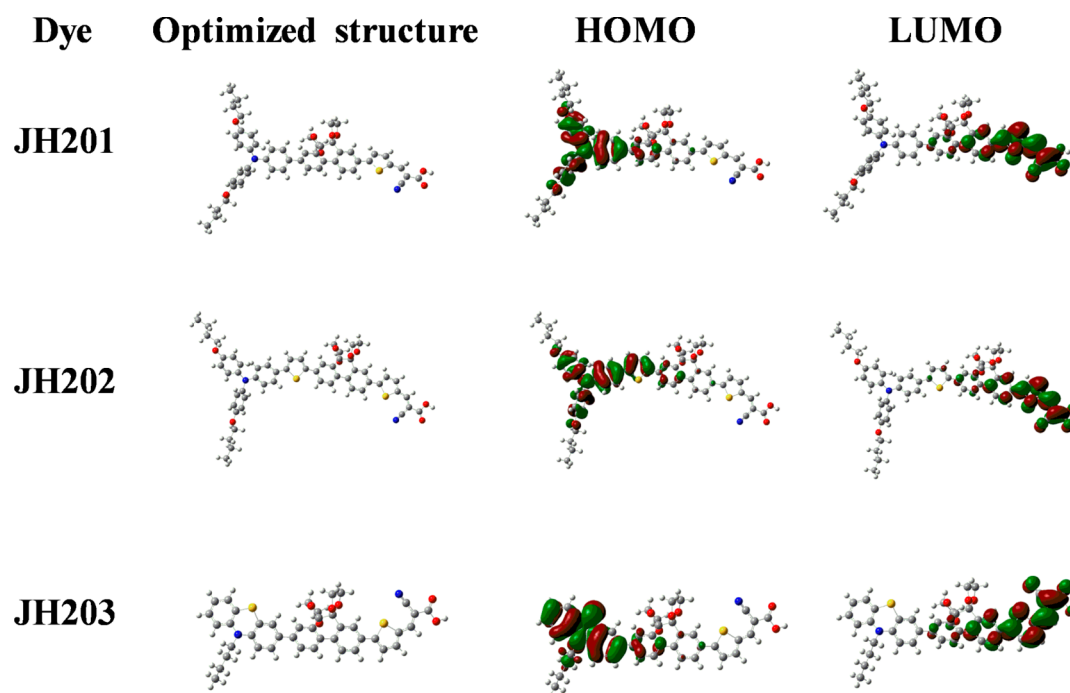


Figure 2. Optimized structures and electron distribution in the highest occupied molecular orbital (HOMO) and lowest unoccupied molecular orbital (LUMO) levels of the **JH** series of the dyes.

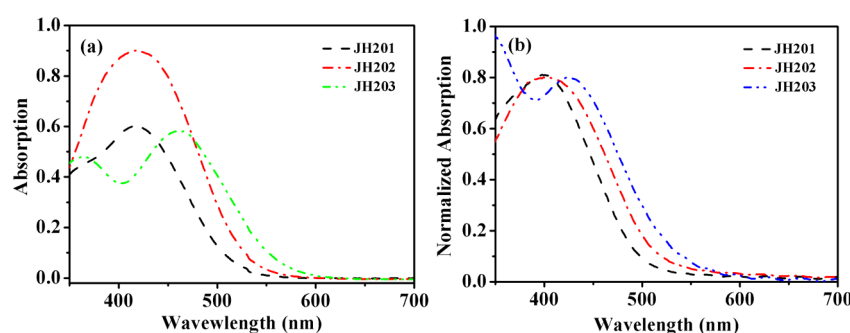


Figure 3. Absorption spectra of **JH201–JH203** in CH_2Cl_2 solution (a) and on TiO_2 films (b).

transition. Upon the addition of a thiophene unit between the electron donor and phenanthrenequinone derivative bridge, dye **JH202** displays a similar absorption wavelength at 420 nm. However, the molar extinction coefficient (λ_{max}) increased from $30155 \text{ M}^{-1}\cdot\text{cm}^{-1}$ for dye **JH201** to $45105 \text{ M}^{-1}\cdot\text{cm}^{-1}$ for dye **JH202**, indicating that dye **JH202** exhibits a stronger light-harvesting ability than dye **JH201**. The reason for this change is due to the introduction of the thiophene unit, diminishing the rotation of the dye molecule, allowing for better delocalization of π -electrons. Unlike the absorption bands of dye **JH201** and dye **JH202**, dye **JH203** exhibits a maximal absorption wavelength of 460 nm with a bathochromic shift of around 40 nm, which is probably due to the stronger electron-donating ability of phenothiazine.²²

Figure 3(b) shows the normalized absorption spectra of the dyes adsorbed on TiO_2 films. Compared to the absorption spectra in solution, a hypochromic shift of 20, 20, and 29 nm was observed for dye **JH201**, dye **JH202**, and dye **JH203**, respectively. This phenomenon is mainly caused by the H-typed aggregation of the dyes.²³ It appears to be a common phenomenon for D- π -A structured organic dyes.^{24–26} We can

conclude that the absorption property of dyes on TiO_2 films can be affected by different electron donors.

Cyclic voltammetry was performed to study the electrochemical properties of the **JH** series of the dyes. The corresponding data are displayed in Table 1. The HOMO levels of all dyes are more positive than I^-/I_3^- (0.4 V vs NHE),²⁷ indicating that the oxidized state dyes can be regenerated effectively by the electrolyte. The LUMO levels of the **JH** series of the dyes are all more negative than the conduction band of TiO_2 (−0.5 V vs NHE),²⁸ implying that the excited dyes can inject an electron to TiO_2 thermodynamically. 4-*tert*-Butylpyridine (TBP) was added to the electrolyte solution to raise the E_{cb} of TiO_2 for obtaining a higher open-circuit voltage (V_{oc}).

The optimized geometries of **JH201–JH203** were obtained using density functional theory (DFT) calculation at the B3LYP/6-31G(d) level.²⁹ The results are shown in Figure 2. According to the optimized structure, it can be noted that the HOMO levels of all the dyes are distributed along the π system covering the electron donor and part of the spacer. The LUMO levels of all dyes are concentrated on the cyanoacetic unit and the part of the spacer. The overlapping of the HOMO and the

LUMO orbitals of the dyes will facilitate the electron transfer from the donor to the acceptor group. It can be noted that for dye **JH202** the rotation between the butoxyltriphenylamine unit and the π -bridge has been reduced in comparison with **JH201**, which are also supported by the higher molar extinction coefficient of **JH202**.

Photovoltaic Properties. The current density–voltage of DSSCs based on the **JH** series of the dyes was evaluated under standard AM 1.5G illumination, and the curves are given in Figure 4. The detailed data are collected in Table 2. The DSSCs

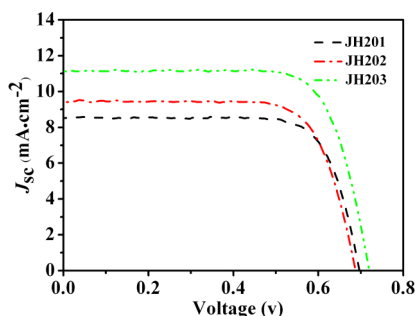


Figure 4. J – V curves of the devices sensitized by **JH201**–**JH203**.

Table 2. Photovoltaic Performance^a of DSSCs Based on the **JH** Series of the Dyes

dye ^b	J_{sc} (mA/cm ²)	V_{oc} (mV)	ff (%)	η (%)
JH201	8.5 ± 0.2	697 ± 10	75.9 ± 0.5	4.5 ± 0.1
JH202	9.4 ± 0.3	688 ± 1	73.7 ± 0.7	4.8 ± 0.1
JH203	11.1 ± 0.1	720 ± 3	74.9 ± 0.3	6.0 ± 0.1

^aIrradiation light: AM 1.5G simulated solar light at room temperature. Working area: 0.159 cm². Electrolyte: 0.6 M DMPII, 0.06 M LiI, 0.4 M TBP, 0.02 M I₂ in dry acetonitrile (AN). ^bThe **JH** series of the dyes were sensitized in 2×10^{-4} M solution in CH₂Cl₂.

based on dye **JH201** exhibit a J_{sc} of 8.5 mA/cm², a V_{oc} of 697 mV, and a ff of 75.9%, corresponding to a η of 4.5%. Upon the introduction of the thiophene unit, the device based on dye **JH202** shows a short-circuit density of 9.4 mA/cm², a V_{oc} of 688 mV, and a ff of 73.7%, corresponding to a η of 4.8%. The increase of short-circuit density for dye **JH202** compared to dye **JH201** is most probably due to the broadened absorption response and the higher molar extinction coefficient. Compared to dye **JH201**, upon the incorporation of the phenothiazene instead of the butoxyltriphenylamine, the device sensitized by dye **JH203** produces an impressive efficiency of 6.0% with a J_{sc} of 11.1 mA/cm², a V_{oc} of 720 mV, and a ff of 74.9%. The explanation for the higher short-current density of dye **JH203** can be mainly attributed to the absorption in the longer-wavelength region when compared to dye **JH201**. The integrated current density curves of the **JH** series of the dyes are shown in Figure 5, which are in agreement with J_{sc} data in Table 2.

The IPCE spectra of dye **JH201**, **JH202**, and **JH203** are shown in Figure 5. The highest IPCE values of 80%, 82%, and 87% were achieved for DSSCs based on dye **JH201**, dye **JH202**, and dye **JH203**, respectively. The IPCE spectrum for the device based on dye **JH202** is a little bit broader and higher than that of **JH201**, which is in agreement with the absorption spectrum, indicating that a well π -conjugated structure is beneficial to the absorption property. Moreover, compared to the device sensitized by dye **JH201**, the dye **JH203**-based

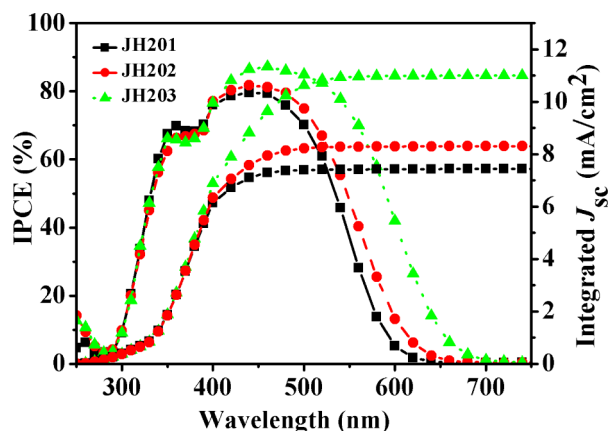


Figure 5. IPCE spectra and integrated current density of the DSSCs based on the **JH** series of the dyes.

device exhibits an evidently widened and higher IPCE spectrum, which favors higher conversion efficiency. As a result, it is a better choice to use the phenothiazine unit as the electron donor rather than the butoxyltriphenylamine unit for higher efficiency in the phenanthrenequinone-bridged metal-free organic dyes in this study.

Electrochemical impedance spectroscopy (EIS) analysis³⁰ was employed to understand the interface charge transfer processes of the DSSCs based on the **JH** series of the dyes. Nyquist plots are shown in Figure 6. It can be seen from the

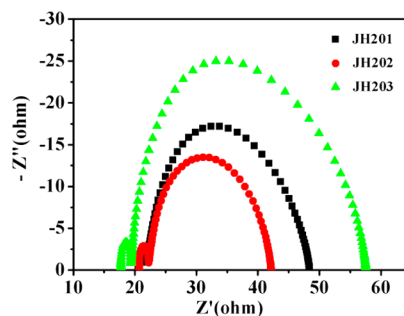


Figure 6. Nyquist plots of DSSCs based on **JH** series of the dyes.

Nyquist plots that the diameters of the larger semicircles in midfrequency area are 26.4, 19.7, and 37.9 Ω /cm² for dye **JH201**, dye **JH202**, and dye **JH203**, respectively. As it is known the diameter in midfrequency represents the electron recombination between TiO₂ and electrolyte. For the **JH** series of the dyes, it can be noted that the recombination resistance (R_{rec}) on the TiO₂/electrolyte interface is increased in the order of **JH202** < **JH201** < **JH203**, which is in accordance with the V_{oc} listed in Table 2.

Stability Test. Stability tests were performed on dye **JH201** based devices in glass boxes under sunlight for 20 days. The electrolyte is composed of 0.6 M DMPII, 0.28 M TBP, 0.04 M I₂, 0.25 M LiI, and 0.05 M GuSCN in 3-methoxy-propanionitrile. As is shown in Figure 7, the device exhibits a stable η and J_{sc} . The V_{oc} has a little decrease, but the loss was compensated by an improvement of ff. Due to the different electrolyte component and the use of 3-methoxy-propanionitrile with a large viscosity in stability test, the dye **JH201** based device yields a lower efficiency than the corresponding data listed in Table 2.

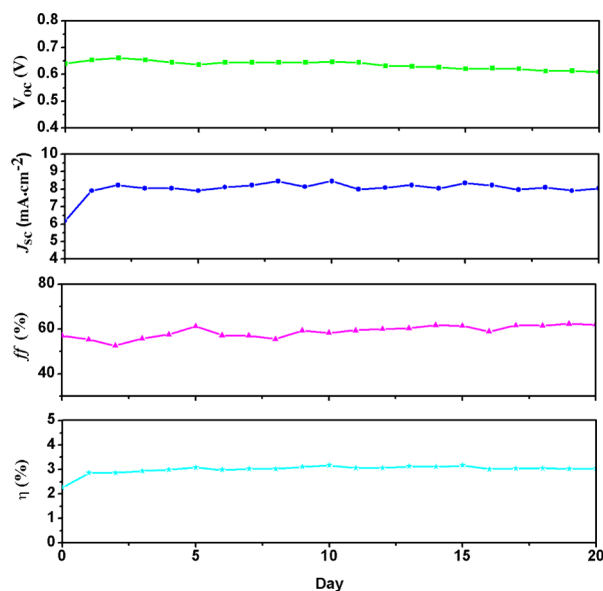


Figure 7. Variation of the photovoltaic parameters (V_{oc} , J_{sc} , ff , and η) with aging time of DSSCs based on JH201 under sunlight.

CONCLUSION

In summary, a series of phenanthrenequinone derivative organic dyes have been designed and synthesized. UV–visible spectrum indicates that dye JH202 shows the highest molar extinction coefficient compared to dye JH201 and dye JH203 due to the introduction of the thiophene unit between the electron donor and phenanthrenequinone derivative π -conjugated bridge. Moreover, dye JH203 exhibits a bathochromic shift of 40 nm compared to dye JH201 and dye JH202, which is probably due to phenothiazine having a stronger electron-donating ability than butoxytriphenylamine. When adsorbed on TiO_2 films, all JH series of the dyes show a hypochromic shift in the range of 20–30 nm. Electrochemical studies provide evidence for the effective electron injection and regeneration of JH series of the dyes. When applied in DSSCs, dye JH203 exhibits the highest efficiency of 6.0% due to the better absorption property compared to dye JH201 and dye JH202. This work helps display the importance of molecule engineering in designing highly efficient organic dyes used in DSSCs.

ASSOCIATED CONTENT

Supporting Information

The detailed synthetic routes and characteristics of the synthesized compounds. This material is available free of charge via the Internet at <http://pubs.acs.org>.

AUTHOR INFORMATION

Corresponding Author

*E-mail: yangxc@dlut.edu.cn. Fax: +86 411 84986250. Tel.: +86 411 84986247. E-mail: lichengs@kth.se. Fax: +46-8-791-2333.

Notes

The authors declare no competing financial interest.

ACKNOWLEDGMENTS

We gratefully acknowledge the financial support of this work from China Natural Science Foundation (Grant 21076039, Grant 21276044, Grant 21120102036 and 20923006), the National Basic Research Program of China (Grant No.

2009CB220009), the Swedish Energy Agency, K&A Wallenberg Foundation, and the State Key Laboratory of Fine Chemicals (KF0805), the Program for Innovative Research Team of Liaoning Province (Grant No. LS2010042).

REFERENCES

- (1) O'Regan, B.; Grätzel, M. A Low-Cost, High-Efficiency Solar Cell Based on Dye-Sensitized Colloidal TiO_2 Films. *Nature* **1991**, *353*, 737–740.
- (2) Nazeeruddin, M. K.; Zakeeruddin, S. M.; Humphry-Baker, R.; Jirousek, M.; Liska, P.; Vlachopoulos, N.; Shklover, V.; Fischer, C.-H.; Grätzel, M. Acid–Base Equilibria of (2,2'-Bipyridyl-4,4'-dicarboxylic acid)ruthenium(II) Complexes and the Effect of Protonation on Charge-Transfer Sensitization of Nanocrystalline Titania. *Inorg. Chem.* **1999**, *38*, 6298–6305.
- (3) Funaki, T.; Funakoshi, H.; Kitao, O.; Komatsuzaki, N. O.; Kasuga, K.; Sayama, K.; Sugihara, H. Cyclometalated Ruthenium(II) Complexes as Near-IR Sensitizers for High Efficiency Dye-Sensitized Solar Cells. *Angew. Chem., Int. Ed.* **2012**, *51*, 7528–7531.
- (4) Yella, A.; Lee, H. W.; Tsao, H. N.; Yi, C.; Chandiran, A. K.; Nazeeruddin, M. K.; Diau, E. W. G.; Yeh, C. Y.; Zakeeruddin, S. M.; Grätzel, M. Porphyrin-Sensitized Solar Cells with Cobalt (II/III)-Based Redox Electrolyte Exceed 12% Efficiency. *Nature* **2011**, *334*, 629–634.
- (5) Zeng, W.; Cao, Y.; Bai, Y.; Wang, Y.; Shi, Y.; Zhang, M.; Wang, F.; Pan, C.; Wang, P. Efficient Dye-Sensitized Solar Cells with an Organic Photosensitizer Featuring Orderly Conjugated Ethylenedioxythiophene and Dithienosilole Blocks. *Chem. Mater.* **2010**, *22*, 1915–1925.
- (6) Tsao, H. N.; Yi, C.; Moehl, T.; Yum, J. H.; Zakeeruddin, S. M.; Nazeeruddin, M. K.; Grätzel, M. Cyclopentadithiophene Bridged Donor–Acceptor Dyes Achieve High Power Conversion Efficiencies in Dye-Sensitized Solar Cells Based on the *tris*-Cobalt Bipyridine Redox Couple. *ChemSusChem* **2011**, *4*, 591–594.
- (7) Do, K.; Kim, D.; Cho, N.; Paek, S.; Song, K.; Ko, J. New Type of Organic Sensitizers with a Planar Amine Unit for Efficient Dye-Sensitized Solar Cells. *Org. Lett.* **2012**, *14*, 222–225.
- (8) Hagberg, D. P.; Edvinsson, T.; Marinado, T.; Boschloo, G.; Hagfeldt, A.; Sun, L. A Novel Organic Chromophore for Dye-Sensitized Nanostructured Solar Cells. *Chem. Commun.* **2006**, *21*, 2245–2247.
- (9) Tian, H.; Yang, X.; Chen, R.; Zhang, R.; Hagfeldt, A.; Sun, L. Effect of Different Dye Baths and Dye Structures on the Performance of Dye-Sensitized Solar Cells Based on Triphenylamine Dyes. *J. Phys. Chem. C* **2008**, *112*, 11023–11033.
- (10) Kitamura, T.; Ikeda, M.; Shigaki, K.; Inoue, T.; Anderson, N. A.; Lian, T.; Yanagida, S. Phenyl-Conjugated Oligoene Sensitizers for TiO_2 Solar Cells. *Chem. Mater.* **2004**, *16*, 1806–1812.
- (11) Tian, H.; Yang, X.; Chen, R.; Li, L.; Hagfeldt, A.; Sun, L. Phenothiazine Derivatives for Efficient Organic Dye-Sensitized Solar Cells. *Chem. Commun.* **2007**, *36*, 3741–3743.
- (12) Hara, K.; Sayama, K.; Ohga, Y.; Shinpo, A.; Suga, S.; Arakawa, H. A Coumarin-Derivative Dye Sensitized Nanocrystalline TiO_2 Solar Cell Having a High Solar-Energy Conversion Efficiency up to 5.6%. *Chem. Commun.* **2001**, *6*, 569–570.
- (13) Wang, Z. S.; Cui, Y.; Hara, K.; Dan-Oh, Y.; Kasada, C.; Shinpo, A. A High-Light-Harvesting-Efficiency Coumarin Dye for Stable Dye-Sensitized Solar Cells. *Adv. Mater.* **2007**, *19*, 1138–1141.
- (14) Hara, K.; Wang, Z.; Sato, T.; Furube, A.; Katoh, R.; Sugihara, H.; Dan-oh, Y.; Kasada, C.; Shinpo, A.; Suga, S. Oligothiophene-Containing Coumarin Dyes for Efficient Dye-Sensitized Solar Cells. *J. Phys. Chem. B* **2005**, *109*, 15476–15482.
- (15) Zhu, W.; Wu, Y.; Wang, S.; Li, W.; Li, X.; Chen, J.; Wang, Z. S.; Tian, H. Organic D-A- π -A Solar Cell Sensitizers with Improved Stability and Spectral Response. *Adv. Funct. Mater.* **2011**, *21*, 756–763.
- (16) Liu, B.; Zhu, W.; Zhang, Q.; Wu, W.; Xu, M.; Ning, Z.; Xie, Y.; Tian, H. Conveniently Synthesized Isophorone Dyes for High Efficiency Dye-Sensitized Solar Cells: Tuning Photovoltaic Perform-

ance by Structural Modification of Donor Group in Donor- π -Acceptor System. *Chem. Commun.* **2009**, 13, 1766–1768.

(17) Kuang, D.; Uchida, S.; Humphry-Baker, R.; Zakeeruddin, S. M.; Grätzel, M. Organic Dye-Sensitized Ionic Liquid Based Solar Cells: Remarkable Enhancement in Performance through Molecular Design of Indoline Sensitizers. *Angew. Chem., Int. Ed.* **2008**, 47, 1923–1927.

(18) He, J.; Guo, F.; Li, X.; Wu, W.; Yang, J.; Hua, J. New Bithiazole-Based Sensitizers for Efficient and Stable Dye-Sensitized Solar Cells. *Chem.—Eur. J.* **2012**, 18, 7903–7915.

(19) Liu, B.; Wang, R.; Mi, W.; Li, X.; Yu, H. Novel Branched Coumarin Dyes for Dye-Sensitized Solar Cells: Significant Improvement in Photovoltaic Performance by Simple Structure Modification. *J. Mater. Chem.* **2012**, 22, 15379–15387.

(20) Xu, M.; Zhang, M.; Pastore, M.; Li, R.; Angelis, F. D.; Wang, P. Joint Electrical, Photophysical and Computational Studies on D- π -A Dye Sensitized Solar Cells: the Impacts of Dithiophene Rigidification. *Chem. Sci.* **2012**, 3, 976–983.

(21) Teng, C.; Yang, X.; Yang, C.; Li, S.; Cheng, M.; Hagfeldt, A.; Sun, L. Molecular Design of Anthracene-Bridged Metal-Free Organic Dyes for Efficient Dye-Sensitized Solar Cells. *J. Phys. Chem. C* **2010**, 114, 9101–9110.

(22) Tian, H.; Yang, X.; Cong, Y.; Chen, R.; Liu, J.; Hao, Y.; Wang, L.; Sun, L. Effect of Different Electron Donating Groups on the Performance of Dye-Sensitized Solar Cells. *Dyes Pigm.* **2010**, 84, 62–68.

(23) Khazraji, A. C.; Hotchandani, S.; Das, S.; Kamat, P. V. Controlling Dye (Merocyanine-540) Aggregation on Nanostructured TiO₂ Films. An Organized Assembly Approach for Enhancing the Efficiency of Photosensitization. *J. Phys. Chem. B* **1999**, 103, 4693–4700.

(24) Yang, C. J.; Chang, Y. J.; Watanabe, M.; Hon, Y. S.; Chow, T. J. Phenothiazine Derivatives as Organic Sensitizers for Highly Efficient Dye-Sensitized Solar Cells. *J. Mater. Chem.* **2012**, 22, 4040–4049.

(25) Kim, S.; Choi, H.; Kim, D.; Song, K.; Kang, S. O.; Ko, J. Novel Conjugated Organic Dyes Containing Bis-Dimethylfluorenyl Amino Phenyl Thiophene for Efficient Solar Cell. *Tetrahedron* **2007**, 63, 9206–9212.

(26) Sayama, K.; Hara, K.; Mori, N.; Satsuki, M.; Suga, S.; Tsukagoshi, S.; Abe, Y.; Sugihara, H.; Arakawa, H. Photosensitization of a Porous TiO₂ Electrode with Merocyanine Dyes Containing a Carboxyl Group and a Long Alkyl Chain. *Chem. Commun.* **2000**, 13, 1173–1174.

(27) Hara, K.; Sato, T.; Katoh, R.; Furube, A.; Yoshihara, T.; Murai, M.; Kurashige, M.; Ito, S.; Shinpo, A.; Suga, S.; et al. Novel Conjugated Organic Dyes for Efficient Dye-Sensitized Solar Cells. *Adv. Funct. Mater.* **2005**, 15, 246–252.

(28) Boschloo, G.; Hagfeldt, A. Activation Energy of Electron Transport in Dye-Sensitized TiO₂ Solar Cells. *J. Phys. Chem. B* **2005**, 109, 12093–12098.

(29) Frisch, M.; Trucks, G.; Schlegel, H.; Scuseria, G.; Robb, M.; Cheeseman, J. *Gaussian 03*, Revision C.02; Gaussian, Inc.: Wallingford, CT, 2004.

(30) Wang, Z.; Koumura, N.; Cui, Y.; Takahashi, M.; Sekiguchi, H.; Mori, A.; Kubo, T.; Furube, A.; Hara, K. Hexylthiophene-Functionalized Carbazole Dyes for Efficient Molecular Photovoltaics: Tuning of Solar-Cell Performance by Structural Modification. *Chem. Mater.* **2008**, 20, 3993–4003.